ACS Energy LETTERS

http://pubs.acs.org/journal/aelccp

Moisture Uptake Relaxes Stress in Metal Halide Perovskites at the Expense of Stability

Gabriel R. McAndrews,△ Boyu Guo,△ Samantha C. Kaczaral,△ Karen Fukuda, Matteo R. S. Poma, Rebecca A. Belisle, Aram Amassian,* and Michael D. McGehee*

Cite This: *ACS Energy Lett.* 2024, 9, 4153−4161

Read Online

ACCESS | Metrics & More | Article Recommendations | Supporting Information

ABSTRACT: Previous studies have shown that the degradation rate of metal halide perovskites in an ambient atmosphere increases with the amount of tensile stress, which primarily arises from the coefficient of thermal expansion mismatch with the substrate. In this work, we show the first evidence of tensile stress relaxation in perovskite films resulting from moisture uptake. Indeed, for multiple perovskite compositions we observe that tension relaxes rapidly in ambient conditions, as compared to inert conditions, with quartz crystal microbalance measurements showing a mass density increase on a similar time scale indicative of moisture uptake. The uptake of moisture at free surfaces, including grain boundaries, can reduce tension in a constrained film, similar to how adatom diffusion reduces residual stress following thin film formation. Unfortunately, the uptake of moisture can catalyze other degradation mechanisms such as PbI_2 formation or a transition to a nonperovskite structural phase. Stress-induced uptake of moisture is an especially important problem for all-inorganic perovskites because they are annealed at much higher temperatures, causing high tensile stress. It explains the unusually poor ambient stability of these perovskites. Using a diethyl ether antisolvent bath to attach $CsPbI_2Br$ to the substrate at a much lower temperature, we reduced the initial tensile strain from 0.43 ± 0.04% to 0.12 ± 0.05%, thus reducing the driving force for moisture uptake and improving its ambient phase stability by over a factor of 15.

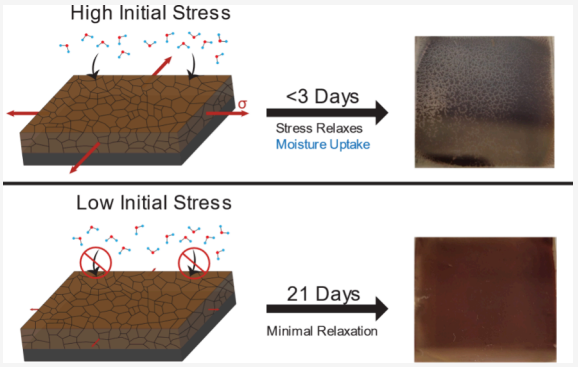

Perovskite photovoltaics would benefit from further improvements in the operational stability given their promising power conversion efficiencies of single junction cells (>26%) and tandems (33.9%).[1] Environmental factors, such as light, heat, moisture, and oxygen, can accelerate perovskite degradation with the formation of PbI_2,[2] reduction/oxidation reactions that form Pb(0) and I_2 (gas),[3−6] structural rearrangements into nonphotoactive materials,[7] or the release of volatile organic components.[8] Several effective methods to improve stability include the use of redox shuttles to reverse halide oxidation/metal reduction,[9,10] physical barrier layers to prevent oxygen/moisture ingress,[11] and grain boundary and surface passivation to nullify the reactivity of defects.[12]

Thin film stress, and specifically tension, has been shown to accelerate degradation mechanisms and leaves brittle perovskites susceptible to fracture and delamination.[13−16] Recent reviews and studies highlight the importance of stress manipulation as an effective strategy to improve perovskite solar cell stability and mechanical reliability.[17−22] While there are several sources for intrinsic stress development during a solution process, such as grain coalescence,[23] the coefficient of thermal expansion (CTE) mismatch between the perovskite and underlying substrate is often the largest contributor to the perovskite's in-plane, biaxial tension.[13,24] The expected thermal stress in the perovskite is expressed as[25]

$$\sigma_{\Delta T} = \frac{E_f}{1-\nu_f}\varepsilon_{\Delta T} = \frac{E_f}{1-\nu_f}(\alpha_s - \alpha_f)(T - T_{ref}) \quad (1)$$

where E_f is the Young's modulus of the perovskite film, ν_f is the Poisson's ratio of the perovskite film, $\varepsilon_{\Delta T}$ is the thermal strain, α_s is the CTE of the substrate, α_f is the CTE of the perovskite film, T is the current temperature, and T_{ref} is the temperature where zero thermal strain is present in the perovskite.[24,25]

T_{ref} is conceptualized as the temperature at which the perovskite structure mechanically attaches to the underlying substrate. While T_{ref} depends heavily on the perovskite

Received: July 4, 2024
Accepted: July 23, 2024
Published: July 30, 2024

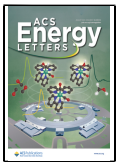

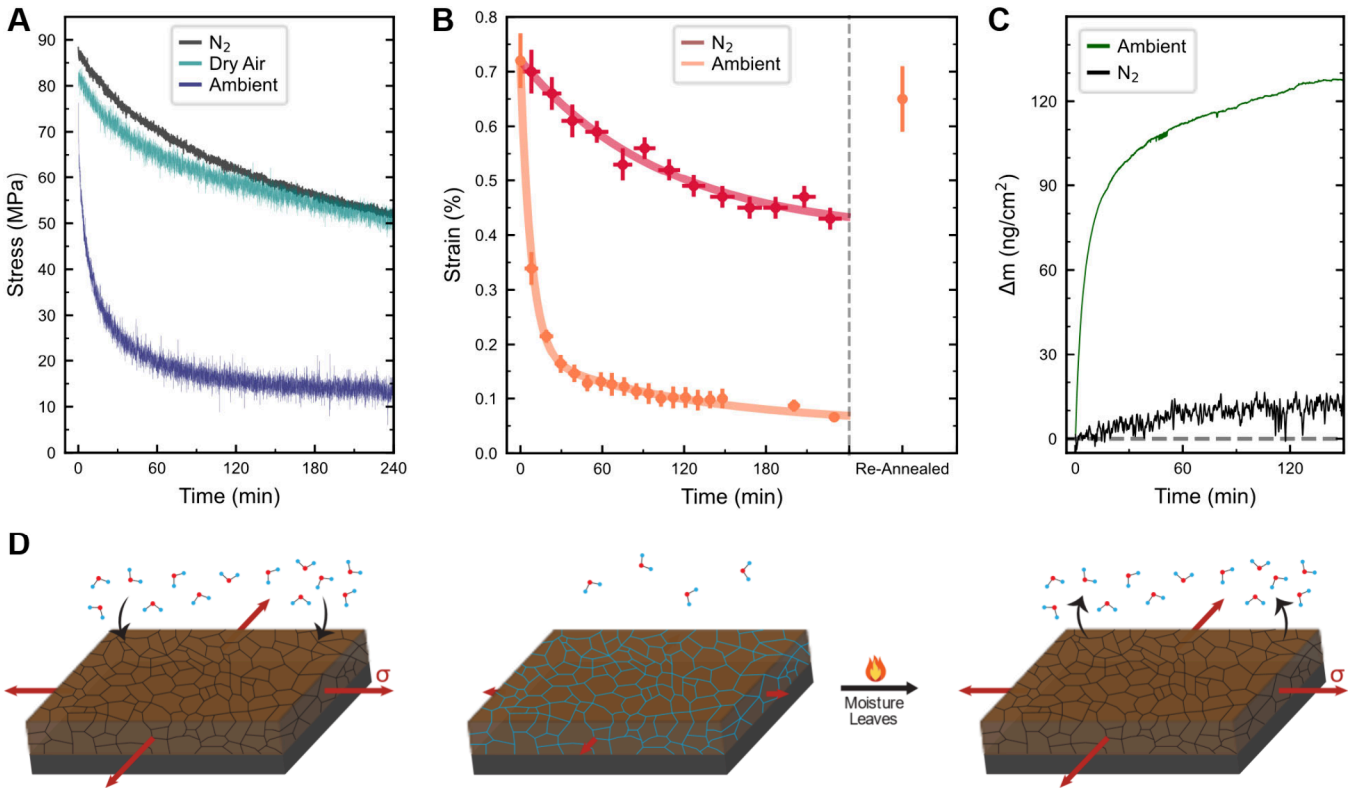

Figure 1. (A) Stress versus time for $FAPbBr_3$ on a silicon substrate in inert (black) (N_2, dark, 25 °C, <1% relative humidity), dry air (teal) (dark, 25 °C, <1% relative humidity), and ambient (blue) (dark, 25 °C, 30−35% relative humidity) environments. Stress measured with a multibeam optical sensor (MOS) laser substrate curvature system. (B) Strain versus time for $FAPbBr_3$ on a silicon substrate in inert (red) (N_2, dark, 23 °C, <0.1 ppm of H_2O) and ambient (orange) (dark, 23 °C, 25−30% relative humidity) environments. Strain increases after reannealing (150 °C for 20 min) and cooling back to room temperature. Strain measured with the XRD:$\sin^2\psi$ method. (C) Mass density change of $FAPbBr_3$ versus time in ambient conditions (green) (dark, 25 °C, 25−30% relative humidity) and in N_2 (black) (dark, 25 °C, <1% relative humidity). (D) Schematic of moisture uptake which reduces tension and is reversed by annealing.

composition, ink formulation, and fabrication method, it is also often strongly dependent on the annealing temperature.[24] When perovskite films are cooled from high anneal temperatures (100−350 °C), tension is expected, as the attachment to the underlying substrate prevents the perovskite lattice from intrinsically contracting.[13]

Tension has been linked to poor stability for various perovskite compositions.[13,14,26] For example, Zhao et al. and Rolston et al. independently demonstrated that the formation of PbI_2 occurs faster in perovskite films with externally applied tension compared to films under applied compression for a reduced and elevated moisture environment, respectively. In addition, residual tension in the perovskite film has been linked to accelerated device efficiency decay during long-term stability testing compared to that of residual compression.[17] In traditional metal thin films, tension has been shown to create a driving force for the diffusion of surface adatoms into grain boundaries of a polycrystalline film to relax its stress.[27−29] We posit that residual tension resulting from CTE mismatch during perovskite thin film manufacturing can provide a driving force for the volumetric uptake of environmental adsorbates, such as moisture, which are known to interact with perovskite surfaces.

Here, for the first time, evidence of perovskite stress relaxation in an ambient environment is presented for several perovskite compositions, including $FAPbBr_3$, $MAPbI_3$, and $MAPbBr_3$. Stress relaxation is attributed to the volumetric mass uptake of moisture within the perovskite film (e.g., grain boundaries and internal free surfaces). This observation is used to develop a new framework to understand the relationship between tension and the rapid degradation of perovskites. We hypothesize that the driving force for moisture uptake can be limited by lowering initial tension, which reduces the volumetric uptake of moisture and improves long-term stability. We then test this hypothesis with an inorganic $CsPbI_2Br$ perovskite composition that is notoriously moisture sensitive and show that lowering initial tension significantly improves the perovskite phase stability.

In Figure 1A, we show stress, measured with a multibeam optical sensor (MOS) laser substrate curvature system, for a $FAPbBr_3$ perovskite as a function of time after cooling from an anneal (150 °C) in three environments: ambient (dark, 25 °C, 30−35% relative humidity), N_2 (dark, 25 °C, <1% relative humidity), and dry air (dark, 25 °C, <1% relative humidity). The corresponding strain, separately measured with the XRD:$\sin^2\psi$ method, is shown in Figure 1B for an inert (N_2) and ambient environment (Notes S1 and S2 in the Supporting Information). Tension is initially present in $FAPbBr_3$ (78 MPa stress, 0.73% strain), as expected from the CTE mismatch with the silicon substrate (eq 1), but rapidly decays in an ambient environment. Upon reannealing at 150 °C, the tension in the perovskite film recovers to its prerelaxed value (Figure 1B). For perovskite films in inert (N_2) or dry air environments, a decrease in tension is observed, but at about an order of magnitude slower rate than the relaxation in ambient. A separate work is being prepared to discuss the mechanisms and implications of intrinsic stress relaxation for perovskites in N_2, which is beyond the scope of this study. Exponential fits were applied for stress and strain

https://doi.org/10.1021/acsenergylett.4c01817
ACS Energy Lett. 2024, 9, 4153−4161

relaxation in N_2, dry air, and ambient air, and details can be found in Tables S1−S5. Relaxation data for additional $FAPbBr_3$ samples are shown in Tables S6 and S7 and Figures S4 and S5. Importantly, the eventual steady-state stress (σ_∞) represents a critical threshold, below which relaxation and its corresponding driving mechanism are not predicted to occur. Further, in the ambient environment, this steady-state stress is substantially lower than that in either N_2 or dry air (~47 MPa for N_2 and dry air; ~12 MPa in ambient). Just recently, an initial study of stress relaxation in $MAPbI_3$ in N_2 was published by Samoylov and colleagues.[30] However, to the best of our knowledge, this is the first evidence of reversible perovskite stress relaxation in an ambient environment.

The relaxation in an ambient environment closely resembles the process of diffusional stress relaxation in phosphosilicate glass.[31−34] In this case, moisture sorption onto free surfaces at voids and internal surfaces decreases the tension in the glass. A reduction of surface energy and stress was proposed to be the driving force for moisture adsorption that caused mechanical forces on the glass that would result in intrinsic expansion (swelling) and, therefore, compression when confined. Upon heating, the moisture was released from internal voids and the stress within the phosphosilicate glass returned to its original, prerelaxed state.[31]

For $FAPbBr_3$ in an ambient environment, it appears that a similar phenomenon is responsible for the observed tensile stress and strain decay over time. In fact, a mass density increase of ~110 ng/cm^2 was detected within 60 min of exposure to an ambient environment with quartz crystal microbalance (QCM) measurements (Figure 1C) ($FAPbBr_3$ film thickness ~240 nm). Over the same time only a minimal mass density change was observed in N_2 (<10 ng/cm^2). This change in N_2 could be considered a baseline that accounts for commonly observed drift in QCM systems.[35] The similar relaxation behavior for films in dry air and N_2 indicates that oxygen alone does not significantly contribute to the acceleration of the relaxation mechanism (Figure 1A, Tables S1 and S5). Rapid relaxation toward near-complete elimination of tension is observed only in the presence of moisture. Moisture sorption likely occurs at perovskite free surfaces (e.g., grain boundaries, top interface, voids), and the mass density increase is substantially higher than that required for an adsorbed monolayer on a top interface (~10 ng/cm^2) (Note S3).[36,37] We emphasize that this quantity of moisture uptake is sufficient to cover all external perovskite grain surfaces with an even distribution. The combination of measurements performed in nitrogen, dry air, and ambient conditions shows that water uptake substantially increases the rate and extent of stress relaxation.

Qualitatively, the rate of mass density change closely mirrors the rate of strain and stress relaxation for $FAPbBr_3$ in an ambient environment (Figures S8−S10); within uncertainty the similarity is reflected in the strain decay rate and the inverse decay rate (parameter b for the fit to $\Delta m = A(1 - e^{t/b})$) for mass density (Figure S8, Tables S4, S6, S7, and S11). Several factors complicate the analysis to extract a kinetic model that relates mass uptake to strain relaxation. For one, moisture at free interfaces (i.e., the top perovskite surface) would not contribute to swelling related phenomena and stress relaxation but would still contribute to an observed mass density increase in QCM. Therefore, it is not possible to decouple mass uptake contributions from top surface and intragranular moisture adsorption. In addition, the density of termination sites for adsorption depends on the surface roughness at the atomic scale (e.g., step-edges). Despite these complications, the qualitative similarity between mass uptake and strain as well as the drastic difference in relaxation and mass uptake between moisture-free (N_2 and dry air) and ambient conditions provide evidence that strain and moisture uptake are coupled. As shown in Figure S11, after reannealing $FAPbBr_3$ mass uptake is detected with QCM for all cycles studied. Although the possibility of some moisture remaining upon reannealing cannot be ruled out (Figure S12), the return of tension after reannealing provides a driving force for additional uptake processes to occur.

The proposed stress and strain relaxation process for ambient environments is schematically shown in Figure 1D and is conceptualized in three steps. First, volumetric moisture uptake would cause an unconstrained perovskite film to expand; however, due to the mechanical attachment, a compressive stress contribution develops that counteracts existing tension from the CTE mismatch with the substrate (eq 1). As tension approaches the steady-state stress, the driving force for additional moisture uptake is diminished. Finally, reannealing the perovskite film removes adsorbed moisture and the tension from the CTE mismatch with the substrate returns.

Although $FAPbBr_3$ is scarcely used as a photovoltaic absorber material due to its large bandgap (~2.3 eV),[38,39] this composition was selected to study the details of the relaxation phenomena in perovskites for several reasons. First, several studies have shown that, unlike its iodide-based alternative, $FAPbBr_3$ directly forms the cubic perovskite phase without transient or permanent inclusion of intermediate complexes or secondary phases.[23,40] Second, light-induced halide segregation is avoided, as $FAPbBr_3$ is a single halide composition.[41,42] Lastly, compared with MA-based perovskite compositions, $FAPbBr_3$ is relatively stable in air and under illumination.[43] Due to these characteristics, we are confident that the observed relaxation is not influenced by structural phase transitions or atomic rearrangement processes. Importantly, the relaxation observed here is unique to that reported recently by Ahmad et al. in which stress irreversibly relaxed due to the decomposition of $MAPbI_3$ to nonperovskite phases (i.e., PbI_2).[44] No signs of structural degradation or phase transformations were detected with XRD during air exposure for 4 h (Figure S13). To probe the universality of stress and strain relaxation for perovskites in ambient conditions and its mechanism, we explored additional perovskite compositions including $MAPbBr_3$ and $MAPbI_3$ (Figure S14, Figure 2). As shown in Figures S14 and S15, within 60 min of exposure to an ambient environment, tension in $MAPbBr_3$ exponentially decayed from ~85 to ~27 MPa while mass density increased by ~90 ng/cm^2.

The proposed model for stress relaxation in this work hypothesizes that tension above the steady-state stress provides the driving force for moisture uptake. Therefore, it should follow that perovskite films with minimal initial tension could limit moisture uptake and enhance the ambient stability. This is a new framework through which to interpret previously reported relationships between tension and accelerated degradation of perovskites, especially with moisture present.[13,14] In other studies, Zhao et al. linked tension to accelerated ion migration and an increased rate of degradation for perovskite films under illumination in an inert environment.[14] In this case an ~40 nm polystyrene capping layer was selected as a moisture and oxygen barrier; however, polystyrene might not have been effective at preventing moisture ingress, as it typically exhibits an elevated water vapor transmission rate (>1220 g-mm/(m^2 day)) compared to alternative polymeric moisture barriers (e.g.,

https://doi.org/10.1021/acsenergylett.4c01817
ACS Energy Lett. 2024, 9, 4153−4161

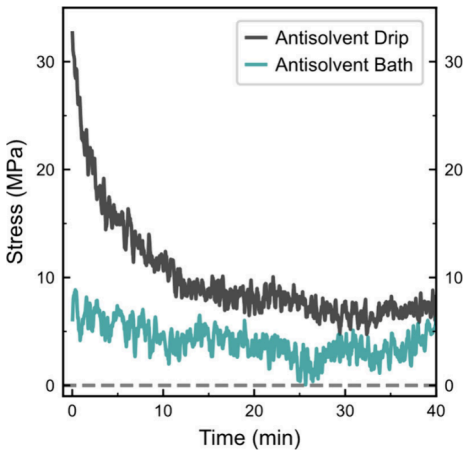

Figure 2. Stress versus time in ambient conditions (dark, 25 °C, ~30% relative humidity) for $MAPbI_3$ on silicon substrates formed with an antisolvent drip (4:1 DMF:DMSO, CB) and with an antisolvent bath (NMP, DEE). Stress was measured with a multibeam optical sensor (MOS) laser substrate curvature system.

PMMA ~55 g-mm/(m^2 day)).[45] So, there remains an opportunity for future work to uncouple the influences of tension driven moisture uptake and increased ion mobility.

To test the hypothesis that moisture uptake is promoted by a tensile stress relaxation mechanism, we first sought to identify the evolution of stress for a perovskite with minimal initial stress. A lower formation temperature should result in a lower attachment temperature and decreased initial tension (eq 1). The antisolvent drip, the classical application of an antisolvent, initiates film nucleation with minimal removal of solution solvent due to the small volume of antisolvent (<200 μL) that is in contact with the film for only seconds. As a result, perovskite films fabricated with the antisolvent drip approach often have elevated tension levels of tension (Figure 2). In contrast, an antisolvent bath removes significantly more solution solvent and can form perovskite films near room temperature.[13] Even after an anneal, the antisolvent bath converted $MAPbI_3$ film has reduced initial stress (<10 MPa) at room temperature due to minimal CTE mismatch driven stress (eq 1) (Figure 2).[13] In ambient conditions, the tension in bath converted $MAPbI_3$ does decrease, but only by ~5 MPa. Further, there is minimal evidence to suggest relaxation drives perovskite stress into compression. Therefore, we hypothesize that minimizing initial stress should limit stress relaxation mechanisms related to moisture uptake.

We aimed to test this hypothesis to improve the ambient stability of a moisture sensitive perovskite composition by manipulating tension, specifically looking at a case study of $CsPbI_2Br$. Cs-based inorganic perovskites require high annealing temperatures and are plagued by poor ambient stability due to interactions with moisture. For example, the perovskite phase of $CsPbI_3$ is thermodynamically unstable at room temperature and requires high temperatures (>320 °C) to form the desirable, photoactive cubic perovskite (α) phase.[46−48] As a $CsPbI_3$ thin film cools, it undergoes a phase transition to the thermodynamically favorable nonperovskite orthorhombic (δ) phase near room temperature.[46,49,50] If the perovskite phase of $CsPbI_3$ is stabilized at room temperature, the transition to the δ-phase can be catalyzed by moisture in ambient conditions.[51−53]

The addition of Br, such as $CsPbI_2Br$, lowers the necessary temperature to form the α-phase and improves the phase stability at room temperature.[47] However, the ambient stability of $CsPbI_{3-x}Br_x$, where $x < 1.2$, is poor because the perovskite structure readily converts to the δ-phase in the presence of moisture.[54,55] The time scale of degradation to the δ-phase in ambient conditions ranges from minutes to hundreds of hours due to the extreme dependence on humidity levels.[48,56,57] $CsPbI_2Br$ thin films still have higher annealing temperatures (generally >200 °C) compared to mixed organic/inorganic thin films (<150 °C).[58−61] As such, the expected T_{ref} (eq 1) of $CsPbI_2Br$ should result in elevated tension as compared with that for the mixed organic/inorganic films. In fact, stress for solution processed $CsPbI_2Br$ has been reported to be as high as 150 MPa.[62,63]

High annealing temperatures are necessary to form the perovskite phase in $CsPbI_2Br$ fabrication; however, they result in high tensile stress and a high driving force for moisture uptake under ambient conditions. We hypothesize that the rapid uptake

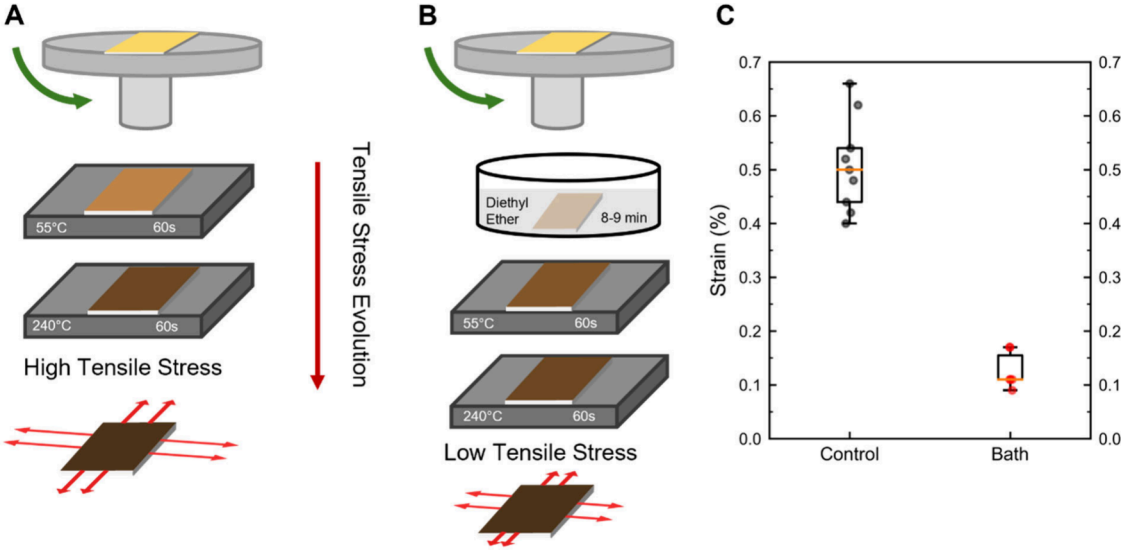

Figure 3. $CsPbI_2Br$ fabrication schematic of the (A) control method and (B) DEE bath method. (C) Summary of initial strain (XRD:$\sin^2\psi$) in thin films made from both fabrication methods. Utilizing a DEE bath significantly lowers the residual tension.

https://doi.org/10.1021/acsenergylett.4c01817
ACS Energy Lett. 2024, 9, 4153−4161

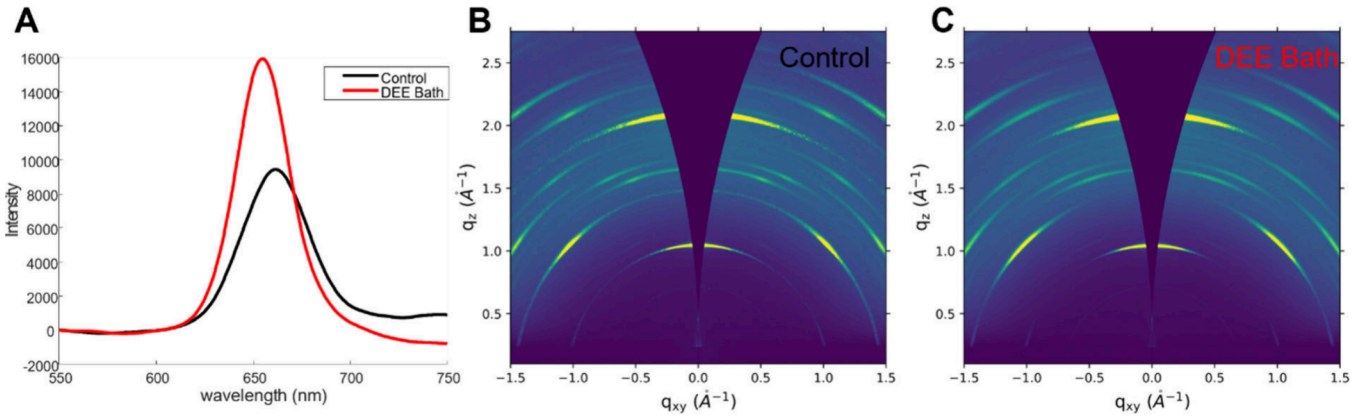

Figure 4. (A) 1 sun photoluminescence comparison of films fabricated via the control and DEE bath methods. GIWAXS patterns of films fabricated with (B) the control method and (C) the DEE bath method.

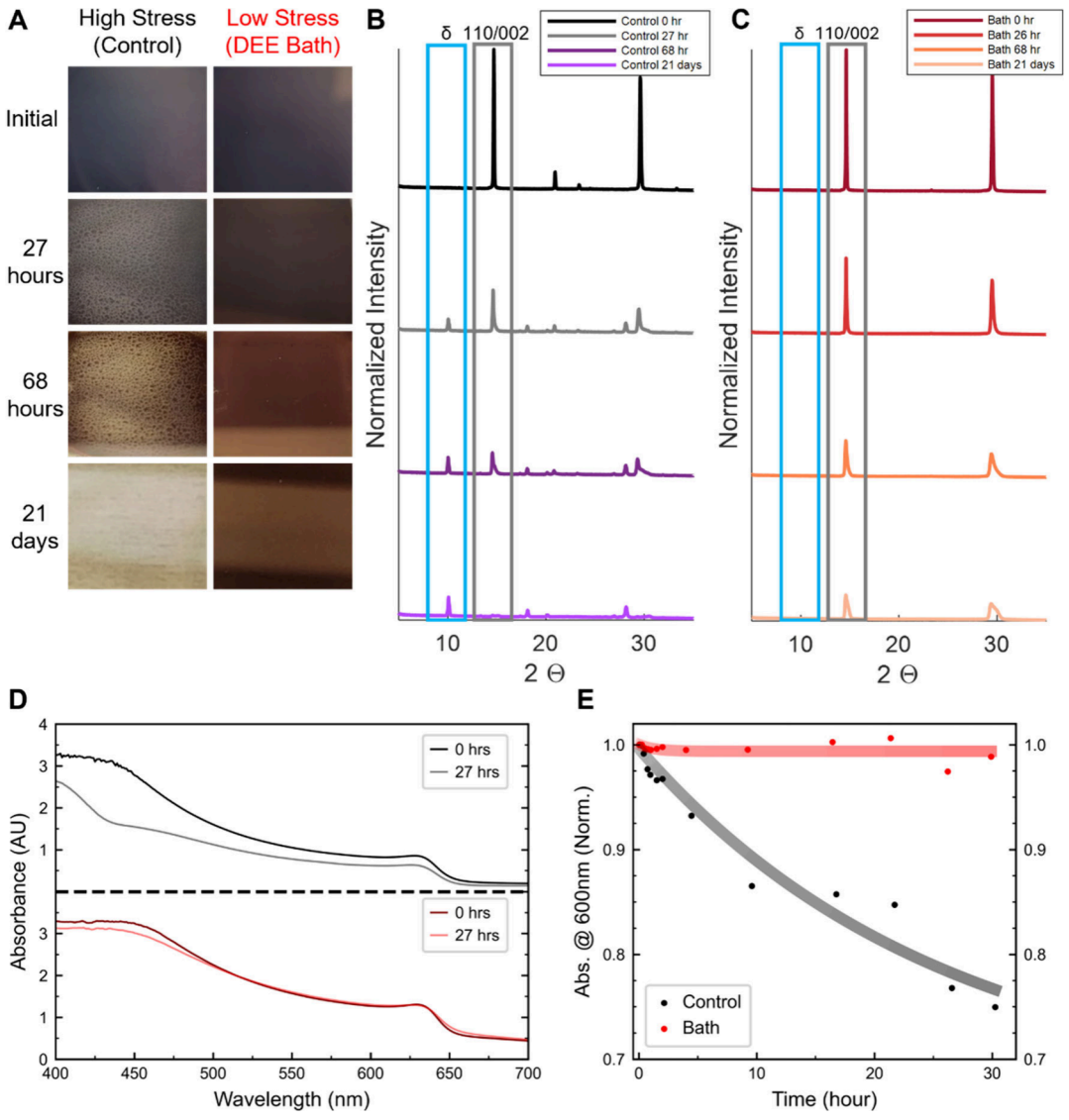

Figure 5. Degradation comparison between control $CsPbI_2Br$ films and DEE bath $CsPbI_2Br$ films using (A) visual signs of δ-phase, (B) XRD of control films, and (C) XRD of DEE bath films. (D) Absorbance spectra comparison of control (black) and bath (red) films. (E) Absorbance versus time comparison at a wavelength of 600 nm.

of moisture to relieve high tensile stress in inorganic perovskite thin films likely contributes to its poor ambient stability. Furthermore, lowering the residual tension will improve the ambient stability. Using our fabrication protocol outlined in the Supporting Information, $CsPbI_2Br$ with annealing temperatures of 55 °C for 60 s followed by 240 °C for 60 s results in an average

https://doi.org/10.1021/acsenergylett.4c01817
ACS Energy Lett. 2024, 9, 4153−4161

tensile stress value of >80 MPa (>0.5% strain) compared to mixed Cs/FA compositions which typically have <50 MPa (<0.3% strain) due to their lower annealing temperatures (Figure S16). In our fabrication of $CsPbI_2Br$, the perovskite salts are dissolved in a mixture of 1:9 (v/v) dimethylformamide (DMF):dimethyl sulfoxide (DMSO). Since DMSO has a higher boiling point compared to DMF (189 °C vs 153 °C), the precursor solvent mixture is less volatile than mixtures with high DMF content. The volatility of the precursor solvent mixture is a determining factor of the perovskite attachment temperature and therefore the residual tension.[24] A low-temperature and high-temperature annealing protocol is used to optimize the nucleation of the perovskite structure, growth of perovskite grains, and solvent evaporation to create a uniform film.[58]

As mentioned earlier, an antisolvent bath is an effective strategy to reduce tension in perovskite thin films.[13] The control and antisolvent bath fabrication methods for $CsPbI_2Br$ are shown in schematic form in Figure 3A,B. In the control method, a brown absorbing phase is not observed until the low-temperature anneal at 55 °C; this phase is likely a dimethyl sulfoxide (DMSO) solvated perovskite structure.[48] However, the introduction of a diethyl ether (DEE) antisolvent bath formed a brown absorbing phase before annealing and initiated attachment at a lower temperature, resulting in lower tensile strain. XRD measurements shown in Figures S17 and S18 confirm a perovskite−solvent phase is formed after the DEE bath, indicating T_{ref} (eq 1) is likely lower for the DEE bath films as a perovskite phase is formed prior to annealing. Initial strain, measured with the XRD:$\sin^2\psi$ method, was reduced from 0.43 ± 0.04% to 0.12 ± 0.05% by using a DEE bath, as shown in Figure 3C. This reduction of strain corresponds to an approximate reduction in tensile stress from 61 ± 6 MPa for the control films to 17 ± 7 MPa in the DEE films (eq 1). For bath converted $CsPbI_2Br$, minimal relaxation (<10 MPa) is observed after 4 h in an ambient environment (Figure S19).

Figure 4 compares the film optoelectronic and structural quality resulting from the control fabrication to that from the DEE bath fabrication. The resulting bandgaps as measured by photoluminescence are similar for the control method and DEE method, 1.88 and 1.89 eV, respectively, as shown in Figure 4A. Grazing incidence wide angle X-ray scattering (GIWAXS) measurements were conducted to compare the crystallographic structure of $CsPbI_2Br$ fabricated using the control method (Figure 4B) and that using the DEE bath method (Figure 4C). Previously, structural degradation into a nonperovskite phase has been linked to specific perovskite crystallographic facets.[64] The integrated GIWAXS and crystallographic orientation analysis comparison in Figure S20 indicate that the fabrication method does not significantly change the perovskite structure of $CsPbI_2Br$, meaning structural differences are not likely to play a major role in variable degradation rates between the two fabrication methods.

To test the ambient stability, three films made with each method were monitored in a laboratory at 21−26.5 °C with 15−29% relative humidity. All films were exposed to the same variable conditions and were measured in parallel. Temperature and relative humidity measurements during the measurement period are reported in Figures S21 and S22. Visual degradation of the control films is evident after only ∼24 h of ambient exposure, as shown in Figure 5A. However, the low stress DEE bath films show little visible δ-phase formation after 3 weeks of ambient exposure. Additional photographs are shown in Figure S23. XRD was used to monitor the degradation of the perovskite since the δ-phase has a distinct diffraction peak at 9.9° 2θ (Cu Kα).[48] XRD patterns as a function of time for the control and DEE bath films are shown in Figure 5B,C, respectively. The degradation of the control film is evident after 24 h of exposure, as the δ-phase peak is present and the perovskite diffraction peaks are asymmetric. However, the DEE bath films do not show any signs of δ-phase growth after 3 weeks of ambient exposure. The DEE bath perovskite diffraction peaks are no longer symmetric after long exposure times, but the perovskite phase has yet to transition to the δ-phase. Additional XRD spectra of multiple samples are shown in Figures S24 and S25. To corroborate the stability results, $CsPbI_2Br$ samples fabricated via both methods were monitored in ambient conditions using *in situ* GIWAXS. While overall degradation occurred at an increased rate due to elevated humidity, the DEE bath films remained in the perovskite phase significantly longer than the control films, as shown in Figure S26.

Absorbance spectroscopy was also used to monitor degradation of the perovskite phase. Figure 5D compares the absorbance spectra before and after 1 day of ambient exposure for the control films and DEE bath films. After ambient exposure, the absorbance of the control film decreased and the δ-phase absorption edge is observed at ∼440 nm. However, the DEE bath film shows consistent absorbance across the tested wavelength range, and no δ-phase absorption edge is detected. The absorbance at 600 nm is tracked as a function of time for control films and DEE bath films as shown in Figure 5E. In the first 24 h of ambient exposure, the control films lose >20% of the initial absorbance as the perovskite structure degrades to the δ-phase. However, the constant absorbance as a function of time for the DEE bath films indicate little degradation occurred. Additional absorbance spectra for multiple samples are shown in Figures S27−S30. The combination of XRD and absorbance measurements confirms visual observation that lowering the tensile stress, with a DEE antisolvent bath, improves ambient stability.

Previous work has shown that morphological changes in perovskite thin films will change water-based degradation.[65−67] We acknowledge that the film formation kinetics and resulting morphology will be altered with the use of an antisolvent bath. To keep the film formation kinetics reasonably similar to the control, the initial tension in the perovskite film was manipulated by using a substrate with a different CTE while using a film formation method identical to that used with glass (Figure 3A). Figure S31 shows scanning electron microscope (SEM) images of films fabricated on glass compared with Kapton showing similar surface features. Kapton has a more closely matched CTE to the perovskite when compared to glass, 40×10^{-6} and 9×10^{-6} K^{-1}, respectively,[68,69] which results in a tensile strain reduction from 0.43 ± 0.04% to 0.27 ± 0.08%, shown in Table S14. The ambient stability of $CsPbI_2Br$ films was improved by over 2.5× compared to films fabricated on glass, as shown in Figures S32 and S33. This further substantiates the hypothesis that reducing the tensile stress reduces water uptake and improves stability.

Through an *in situ* investigation of stress and strain in several perovskite thin film compositions, we have unveiled a new perovskite phenomenon: stress relaxation in ambient environments. QCM measurements indicate that mass uptake occurs over the same time scale as the stress relaxation process. We hypothesized that, like glass materials, tension provides a driving force for moisture uptake and suggest that this mechanism provides a new framework to understand how stress influences

https://doi.org/10.1021/acsenergylett.4c01817
ACS Energy Lett. 2024, 9, 4153−4161

phase stability and perovskite decomposition. Specifically, we speculated that the initial tension in a perovskite film dictates its rate of moisture uptake and therefore its ambient stability. The effectiveness of this new method to improve ambient stability is assessed by lowering the tension in $CsPbI_2Br$, a notoriously moisture sensitive composition. Two different methods were utilized to lower the residual tension: (1) a DEE antisolvent bath which lowers the attachment temperature and (2) fabricating films on Kapton to lower the CTE mismatch. Our analysis suggests that reducing initial tension to decrease the driving force for moisture uptake is a promising strategy to enhance the ambient stability of perovskite photovoltaics: bath converted $CsPbI_2Br$ and $CsPbI_2Br$ fabricated on Kapton exhibit 15-fold and 2.5-fold improvements, respectively, in phase stability compared to high stress control films. The results of this study also emphasize that care should be taken to avoid or account for air exposure when measuring the stress or strain in perovskite films, since nearly complete stress relaxation can occur within hours.

■ ASSOCIATED CONTENT

Supporting Information

The Supporting Information is available free of charge at https://pubs.acs.org/doi/10.1021/acsenergylett.4c01817.

Detailed description of the materials and fabrication methods used, description of $\sin^2\psi$ strain measurements, description of substrate laser curvature stress measurements, and additional stress/strain measurements and stability measurements (PDF)

■ AUTHOR INFORMATION

Corresponding Authors

Aram Amassian − *Department of Materials Science and Engineering, and Organic and Carbon Electronics Laboratories (ORaCEL), North Carolina State University, Raleigh, North Carolina 27695, United States;* orcid.org/0000-0002-5734-1194; Email: aamassi@ncsu.edu

Michael D. McGehee − *Materials Science and Engineering Program and Department of Chemical and Biological Engineering, University of Colorado Boulder, Boulder, Colorado 80303, United States; Renewable and Sustainable Energy Institute (RASEI), University of Colorado Boulder, Boulder, Colorado 80303, United States;* orcid.org/0000-0001-9609-9030; Email: Michael.mcgehee@colorado.edu

Authors

Gabriel R. McAndrews − *Materials Science and Engineering Program, University of Colorado Boulder, Boulder, Colorado 80303, United States*

Boyu Guo − *Department of Materials Science and Engineering, and Organic and Carbon Electronics Laboratories (ORaCEL), North Carolina State University, Raleigh, North Carolina 27695, United States*

Samantha C. Kaczaral − *Department of Chemical and Biological Engineering, University of Colorado Boulder, Boulder, Colorado 80303, United States;* orcid.org/0000-0002-6259-2131

Karen Fukuda − *Physics Department, Wellesley College, Wellesley, Massachusetts 02481, United States*

Matteo R. S. Poma − *Materials Science and Engineering Program, University of Colorado Boulder, Boulder, Colorado 80303, United States*

Rebecca A. Belisle − *Physics Department, Wellesley College, Wellesley, Massachusetts 02481, United States;* orcid.org/0000-0003-2288-150X

Complete contact information is available at: https://pubs.acs.org/10.1021/acsenergylett.4c01817

Author Contributions

△G.R.M., B.G., and S.C.K. contributed equally to this work. Individual author contributions are as follows. G.R.M.: conceptualization, investigation, methodology, validation, writing-original draft, writing-review and editing. B.G.: conceptualization, investigation, methodology, validation, writing-review and editing. S.C.K.: conceptualization, investigation, methodology, validation, writing-original draft, writing-review and editing. K.F.: validation. M.R.S.P.: validation. R.A.B.: validation, writing-review and editing. A.A.: conceptualization, funding acquisition, project administration, supervision, writing-review and editing. M.D.M.: conceptualization, funding acquisition, project administration, supervision, writing-review and editing.

Notes

The authors declare the following competing financial interest(s): M.D.M is an advisor to Swift Solar.

■ ACKNOWLEDGMENTS

This research was funded by the National Science Foundation (NSF) under award number DMR 2245435. This material is based upon work supported by the U.S. Department of Energy's Office of Energy Efficiency and Renewable Energy (EERE) under Solar Energy Technologies Office (SETO) Agreement Number DE-EE0010502. This research was also funded by the Office of Naval Research (ONR) under award number N00014-20-1-2573. This research was supported in part by the Colorado Shared Instrumentation in Nanofabrication and Characterization (COSINC): the COSINC-CHR (Characterization), College of Engineering & Applied Science, University of Colorado Boulder.

■ REFERENCES

(1) Hicks, A. NREL Best Research Cell Efficiencies Chart. https://www.nrel.gov/pv/cell-efficiency.html. (accessed 2024−07−22).

(2) Liang, J.; Hu, X.; Wang, C.; Liang, C.; Chen, C.; Xiao, M.; Li, J.; Tao, C.; Xing, G.; Yu, R.; Ke, W.; Fang, G. Origins and Influences of Metallic Lead in Perovskite Solar Cells. *Joule* **2022**, *6* (4), 816−833.

(3) Alberti, A.; Bongiorno, C.; Smecca, E.; Deretzis, I.; La Magna, A.; Spinella, C. Pb Clustering and PbI2 Nanofragmentation during Methylammonium Lead Iodide Perovskite Degradation. *Nat. Commun.* **2019**, *10* (1), 2196.

(4) Li, N.; Luo, Y.; Chen, Z.; Niu, X.; Zhang, X.; Lu, J.; Kumar, R.; Jiang, J.; Liu, H.; Guo, X.; Lai, B.; Brocks, G.; Chen, Q.; Tao, S.; Fenning, D. P.; Zhou, H. Microscopic Degradation in Formamidinium-Cesium Lead Iodide Perovskite Solar Cells under Operational Stressors. *Joule* **2020**, *4* (8), 1743−1758.

(5) Kerner, R. A.; Xu, Z.; Larson, B. W.; Rand, B. P. The Role of Halide Oxidation in Perovskite Halide Phase Separation. *Joule* **2021**, *5* (9), 2273−2295.

(6) Xu, Z.; Kerner, R. A.; Berry, J. J.; Rand, B. P. Iodine Electrochemistry Dictates Voltage-Induced Halide Segregation Thresholds in Mixed-Halide Perovskite Devices. *Adv. Funct Mater.* **2022**, *32* (33), No. 2203432.

(7) Masi, S.; Gualdrón-Reyes, A. F.; Mora-Seró, I. Stabilization of Black Perovskite Phase in FAPbI3and CsPbI3. *ACS Energy Letters* **2020**, *5* (6), 1974−1985.

(8) Conings, B.; Drijkoningen, J.; Gauquelin, N.; Babayigit, A.; D'Haen, J.; D'Olieslaeger, L.; Ethirajan, A.; Verbeeck, J.; Manca, J.;

Mosconi, E.; De Angelis, F.; Boyen, H. G. Intrinsic Thermal Instability of Methylammonium Lead Trihalide Perovskite. *Adv. Energy Mater.* **2015**, *5* (15), No. 1500477.
(9) Wu, S.; Yan, Y.; Yin, J.; Jiang, K.; Li, F.; Zeng, Z.; Tsang, S. W.; Jen, A. K. Y. Redox Mediator-Stabilized Wide-Bandgap Perovskites for Monolithic Perovskite-Organic Tandem Solar Cells. *Nat. Energy* **2024**, *9*, 411−421.
(10) Wang, L.; Zhou, H.; Hu, J.; Huang, B.; Sun, M.; Dong, B.; Zheng, G.; Huang, Y.; Chen, Y.; Li, L.; Xu, Z.; Li, N.; Liu, Z.; Chen, Q.; Sun, L. D.; Yan, C. H. A Eu 3+ -Eu 2+ Ion Redox Shuttle Imparts Operational Durability to Pb-I Perovskite Solar Cells. *Science (1979)* **2019**, *363* (6424), 265−270.
(11) Johnson, S. A.; White, K. P.; Tong, J.; You, S.; Magomedov, A.; Larson, B. W.; Morales, D.; Bramante, R.; Dunphy, E.; Tirawat, R.; Perkins, C. L.; Werner, J.; Lahti, G.; Velez, C.; Toney, M. F.; Zhu, K.; McGehee, M. D.; Berry, J. J.; Palmstrom, A. F. Improving the Barrier Properties of Tin Oxide in Metal Halide Perovskite Solar Cells Using Ozone to Enhance Nucleation. *Joule* **2023**, *7* (12), 2873−2893.
(12) Zhang, H.; Pfeifer, L.; Zakeeruddin, S. M.; Chu, J.; Grätzel, M. Tailoring Passivators for Highly Efficient and Stable Perovskite Solar Cells. *Nature Reviews Chemistry* **2023**, *7* (9), 632−652.
(13) Rolston, N.; Bush, K. A.; Printz, A. D.; Gold-Parker, A.; Ding, Y.; Toney, M. F.; McGehee, M. D.; Dauskardt, R. H. Engineering Stress in Perovskite Solar Cells to Improve Stability. *Adv. Energy Mater.* **2018**, *8* (29), 1−7.
(14) Zhao, J.; Deng, Y.; Wei, H.; Zheng, X.; Yu, Z.; Shao, Y.; Shield, J. E.; Huang, J. Strained Hybrid Perovskite Thin Films and Their Impact on the Intrinsic Stability of Perovskite Solar Cells. *Science Advances* **2017**, *3* (11), No. eaao5616.
(15) Ramirez, C.; Yadavalli, S. K.; Garces, H. F.; Zhou, Y.; Padture, N. P. Thermo-Mechanical Behavior of Organic-Inorganic Halide Perovskites for Solar Cells. *Scr Mater.* **2018**, *150*, 36−41.
(16) Dai, Z.; Padture, N. P. Challenges and Opportunities for the Mechanical Reliability of Metal Halide Perovskites and Photovoltaics. *Nature Energy* **2023**, *8* (12), 1319−1327.
(17) Muscarella, L. A.; Ehrler, B. The Influence of Strain on Phase Stability in Mixed-Halide Perovskites. *Joule* **2022**, *6* (9), 2016−2031.
(18) Moloney, E. G.; Yeddu, V.; Saidaminov, M. I. Strain Engineering in Halide Perovskites. *ACS Materials Letters* **2020**, *2* (11), 1495−1508.
(19) Tu, Q.; Kim, D.; Shyikh, M.; Kanatzidis, M. G. Mechanics-Coupled Stability of Metal-Halide Perovskites. *Matter* **2021**, *4* (9), 2765−2809.
(20) Wu, J.; Liu, S. C.; Li, Z.; Wang, S.; Xue, D. J.; Lin, Y.; Hu, J. S. Strain in Perovskite Solar Cells: Origins, Impacts and Regulation. *National Science Review* **2021**, *8* (8), No. nwab047.
(21) Dailey, M.; Li, Y.; Printz, A. D. Residual Film Stresses in Perovskite Solar Cells: Origins, Effects, and Mitigation Strategies. *ACS Omega* **2021**, *6* (45), 30214−30223.
(22) Liu, D.; Luo, D.; Iqbal, A. N.; Orr, K. W. P.; Doherty, T. A. S.; Lu, Z. H.; Stranks, S. D.; Zhang, W. Strain Analysis and Engineering in Halide Perovskite Photovoltaics. *Nature Materials* **2021**, *20* (10), 1337−1346.
(23) Guo, B.; Chauhan, M.; Woodward, N. R.; McAndrews, G. R.; Thapa, G. J.; Lefler, B. M.; Li, R.; Wang, T.; Darabi, K.; McGehee, M. D.; Amassian, A. In Situ Stress Monitoring Reveals Tension and Wrinkling Evolutions during Halide Perovskite Film Formation. *ACS Energy Lett.* **2024**, *9* (1), 75−84.
(24) McAndrews, G. R.; Guo, B.; Morales, D. A.; Amassian, A.; McGehee, M. D. How the Dynamics of Attachment to the Substrate Influence Stress in Metal Halide Perovskites. *APL Energy* **2023**, *1* (3), No. 036110.
(25) Stoney, G. G. The Tension of Metallic Films Deposited by Electrolysis. *Proceedings of the Royal Society of London. Series A, Containing Papers of a Mathematical and Physical Character* **1909**, *82* (553), 172−175.
(26) Kennard, R. M.; Dahlman, C. J.; Decrescent, R. A.; Schuller, J. A.; Mukherjee, K.; Seshadri, R.; Chabinyc, M. L. Ferroelastic Hysteresis in Thin Films of Methylammonium Lead Iodide. *Chem. Mater.* **2021**, *33* (1), 298−309.
(27) Gan, D.; Ho, P. S.; Huang, R.; Leu, J.; Maiz, J.; Scherban, T. Isothermal Stress Relaxation in Electroplated Cu Films. I. Mass Transport Measurements. *J. Appl. Phys.* **2005**, *97* (10), No. 103531.
(28) Chen, K.-W.; Hsu, L.-H.; Huang, J.-K.; Wang, Y.-L.; Lo, K.-Y. A Strategic Copper Plating Method Without Annealing Process. *J. Electrochem. Soc.* **2009**, *156* (10), D448.
(29) Thouless, M. D.; Gupta, J.; Harper, J. M. E. Stress Development and Relaxation in Copper Films during Thermal Cycling. *J. Mater. Res.* **1993**, *8* (8), 1845−1852.
(30) Samoylov, A. A.; Dailey, M.; Li, Y.; Lohr, P. J.; Raglow, S.; Printz, A. D. Inelastic Deformation in Methylammonium Lead Iodide Perovskite and Mitigation by Additives during Thermal Cycling. *ACS Energy Lett.* **2024**, *9* (5), 2101−2108.
(31) Von Preissig, F. J.; Nix, W. D. Application of Stress Measurement to the Study of Thermally Activated Processes in Thin-Film Materials. *MRS Proceedings* **1991**, *239* (1), 207−212.
(32) Abadias, G.; Chason, E.; Keckes, J.; Sebastiani, M.; Thompson, G. B.; Barthel, E.; Doll, G. L.; Murray, C. E.; Stoessel, C. H.; Martinu, L. Review Article: Stress in Thin Films and Coatings: Current Status, Challenges, and Prospects. *Journal of Vacuum Science & Technology A: Vacuum, Surfaces, and Films* **2018**, *36* (2), No. 020801.
(33) Hirsch, E. H. Stress in Porous Thin Films through Adsorption of Polar Molecules. *J. Phys. D: Appl. Phys.* **1980**, *13*, 2081.
(34) Scherer, K.; Nouvelot, L.; Lacan, P.; Bosmans, R. Optical and Mechanical Characterization of Evaporated SiO 2 Layers Long-Term Evolution. *Appl. Opt.* **1996**, *35*, 5067.
(35) Easley, A. D.; Ma, T.; Eneh, C. I.; Yun, J.; Thakur, R. M.; Lutkenhaus, J. L. A Practical Guide to Quartz Crystal Microbalance with Dissipation Monitoring of Thin Polymer Films. *J. Polym. Sci.* **2022**, *60* (7), 1090−1107.
(36) Li, Q.; Chen, Z.; Tranca, I.; Gaastra-Nedea, S.; Smeulders, D.; Tao, S. Compositional Effect on Water Adsorption on Metal Halide Perovskites. *Appl. Surf. Sci.* **2021**, *538*, No. 148058.
(37) Lin, S.; Chen, C.; Zhao, L.; Wang, M.; Wang, J.; Zhou, H.; Zhao, C. Molecular Insights into Water Vapor Adsorption and Interfacial Moisture Stability of Hybrid Perovskites for Robust Optoelectronics. *Int. J. Heat Mass Transf* **2021**, *175*, No. 121334.
(38) Liu, Y.; Cai, B.; Yang, H.; Boschloo, G.; Johansson, E. M. J. Solvent Engineering of Perovskite Crystallization for High Band Gap FAPbBr3 Perovskite Solar Cells Prepared in Ambient Condition. *ACS Appl. Energy Mater.* **2023**, *6* (13), 7102−7108.
(39) Jafarzadeh, F.; Castriotta, L. A.; Legrand, M.; Ory, D.; Cacovich, S.; Skafi, Z.; Barichello, J.; De Rossi, F.; Di Giacomo, F.; Di Carlo, A.; Brown, T.; Brunetti, F.; Matteocci, F. Flexible, Transparent, and Bifacial Perovskite Solar Cells and Modules Using the Wide-Band Gap FAPbBr3 Perovskite Absorber. *ACS Appl. Mater. Interfaces* **2024**, *16* (14), 17607−17616.
(40) Wang, K.; Tang, M. C.; Dang, H. X.; Munir, R.; Barrit, D.; De Bastiani, M.; Aydin, E.; Smilgies, D. M.; De Wolf, S.; Amassian, A. Kinetic Stabilization of the Sol−Gel State in Perovskites Enables Facile Processing of High-Efficiency Solar Cells. *Adv. Mater.* **2019**, *31* (32), No. 1808357.
(41) Beal, R. E.; Slotcavage, D. J.; Leijtens, T.; Bowring, A. R.; Belisle, R. A.; Nguyen, W. H.; Burkhard, G. F.; Hoke, E. T.; McGehee, M. D. Cesium Lead Halide Perovskites with Improved Stability for Tandem Solar Cells. *J. Phys. Chem. Lett.* **2016**, *7* (5), 746−751.
(42) Hoke, E. T.; Slotcavage, D. J.; Dohner, E. R.; Bowring, A. R.; Karunadasa, H. I.; McGehee, M. D. Reversible Photo-Induced Trap Formation in Mixed-Halide Hybrid Perovskites for Photovoltaics. *Chem. Sci.* **2015**, *6* (1), 613−617.
(43) Ghasemi, M.; Guo, B.; Darabi, K.; Wang, T.; Wang, K.; Huang, C. W.; Lefler, B. M.; Taussig, L.; Chauhan, M.; Baucom, G.; Kim, T.; Gomez, E. D.; Atkin, J. M.; Priya, S.; Amassian, A. A Multiscale Ion Diffusion Framework Sheds Light on the Diffusion−Stability−Hysteresis Nexus in Metal Halide Perovskites. *Nat. Mater.* **2023**, *22* (3), 329−337.
(44) Ahmad, M.; Cartledge, C.; McAndrews, G.; Giuri, A.; McGehee, M. D.; Rizzo, A.; Rolston, N. Tuning Film Stresses for Open-Air

Processing of Stable Metal Halide Perovskites. *ACS Appl. Mater. Interfaces* **2023**, *15* (44), 51117−51125.
(45) Labware Physical Properties Table. https://assets.thermofisher.com/TFS-Assets/LSG/brochures/D20826.pdf. (accessed 2024−06−25).
(46) Eperon, G. E.; Paternò, G. M.; Sutton, R. J.; Zampetti, A.; Haghighirad, A. A.; Cacialli, F.; Snaith, H. J. Inorganic Caesium Lead Iodide Perovskite Solar Cells. *J. Mater. Chem. A Mater.* **2015**, *3* (39), 19688−19695.
(47) Näsström, H.; Becker, P.; Márquez, J. A.; Shargaieva, O.; Mainz, R.; Unger, E.; Unold, T. Dependence of Phase Transitions on Halide Ratio in Inorganic CsPb(Br: XI1- x)3perovskite Thin Films Obtained from High-Throughput Experimentation. *J. Mater. Chem. A Mater.* **2020**, *8* (43), 22626−22631.
(48) Breniaux, E.; Dufour, P.; Guillemet-Fritsch, S.; Tenailleau, C. Unraveling All-Inorganic CsPbI3 and CsPbI2Br Perovskite Thin Films Formation − Black Phase Stabilization by Cs2PbCl2I2 Addition and Flash-Annealing. *Eur. J. Inorg. Chem.* **2021**, *2021* (30), 3059−3073.
(49) Steele, J. A.; Jin, H.; Dovgaliuk, I.; Berger, R. F.; Braeckevelt, T.; Yuan, H.; Martin, C.; Solano, E.; Lejaeghere, K.; Rogge, S. M. J.; Notebaert, C.; Vandezande, W.; Janssen, K. P. F.; Goderis, B.; Debroye, E.; Wang, Y.-K.; Dong, Y.; Ma, D.; Saidaminov, M.; Tan, H.; Lu, Z.; Dyadkin, V.; Chernyshov, D.; Van Speybroeck, V.; Sargent, E. H.; Hofkens, J.; Roeffaers, M. B. J. Thermal Unequilibrium of Strained Black CsPbI 3 Thin Films. *Science* **2019**, *365* (6454), 679−684.
(50) Kaplan, A. B.; Burlingame, Q. C.; Holley, R.; Loo, Y.-L. Prospects for Inorganic CsPbI 3 Perovskite Solar Cells with Commercially Viable Lifetimes. *APL Energy* **2023**, *1* (1), No. 010901.
(51) Straus, D. B.; Guo, S.; Cava, R. J. Kinetically Stable Single Crystals of Perovskite-Phase CsPbI3. *J. Am. Chem. Soc.* **2019**, *141* (29), 11435−11439.
(52) Lin, J.; Lai, M.; Dou, L.; Kley, C. S.; Chen, H.; Peng, F.; Sun, J.; Lu, D.; Hawks, S. A.; Xie, C.; Cui, F.; Alivisatos, A. P.; Limmer, D. T.; Yang, P. Thermochromic Halide Perovskite Solar Cells. *Nat. Mater.* **2018**, *17* (3), 261−267.
(53) Dastidar, S.; Hawley, C. J.; Dillon, A. D.; Gutierrez-Perez, A. D.; Spanier, J. E.; Fafarman, A. T. Quantitative Phase-Change Thermodynamics and Metastability of Perovskite-Phase Cesium Lead Iodide. *J. Phys. Chem. Lett.* **2017**, *8* (6), 1278−1282.
(54) Sanchez, S.; Christoph, N.; Grobety, B.; Phung, N.; Steiner, U.; Saliba, M.; Abate, A. Efficient and Stable Inorganic Perovskite Solar Cells Manufactured by Pulsed Flash Infrared Annealing. *Adv. Energy Mater.* **2018**, *8* (30), No. 1802060.
(55) Mariotti, S.; Hutter, O. S.; Phillips, L. J.; Yates, P. J.; Kundu, B.; Durose, K. Stability and Performance of CsPbI2Br Thin Films and Solar Cell Devices. *ACS Appl. Mater. Interfaces* **2018**, *10* (4), 3750−3760.
(56) Lim, E. L.; Yang, J.; Wei, Z. Inorganic CsPbI2Br Halide Perovskites: From Fundamentals to Solar Cell Optimizations. *Energy Environ. Sci.* **2023**, *16* (3), 862−888.
(57) Zhu, C.; Lin, F.; Zhang, L.; Xiao, S.; Ma, S.; Liu, S.; Tai, Q.; Zhu, L.; Dai, Q.; Guo, X.; Yang, Y. Understanding the Stability Origins of Ambient Stable CsPbI2Br Inorganic Halide Perovskites. *J. Mater. Chem. A Mater.* **2022**, *10* (24), 13124−13136.
(58) Yan, L.; Xue, Q.; Liu, M.; Zhu, Z.; Tian, J.; Li, Z.; Chen, Z.; Chen, Z.; Yan, H.; Yip, H. L.; Cao, Y. Interface Engineering for All-Inorganic CsPbI2Br Perovskite Solar Cells with Efficiency over 14%. *Adv. Mater.* **2018**, *30* (33), No. 1802509.
(59) Sutton, R. J.; Eperon, G. E.; Miranda, L.; Parrott, E. S.; Kamino, B. A.; Patel, J. B.; Hörantner, M. T.; Johnston, M. B.; Haghighirad, A. A.; Moore, D. T.; Snaith, H. J. Bandgap-Tunable Cesium Lead Halide Perovskites with High Thermal Stability for Efficient Solar Cells. *Adv. Energy Mater.* **2016**, *6* (8), No. 1502458.
(60) Niezgoda, J. S.; Foley, B. J.; Chen, A. Z.; Choi, J. J. Improved Charge Collection in Highly Efficient CsPbBrI2 Solar Cells with Light-Induced Dealloying. *ACS Energy Lett.* **2017**, *2* (5), 1043−1049.
(61) Xu, W.; He, F.; Zhang, M.; Nie, P.; Zhang, S.; Zhao, C.; Luo, R.; Li, J.; Zhang, X.; Zhao, S.; Li, W. Di; Kang, F.; Nan, C. W.; Wei, G. Minimizing Voltage Loss in Efficient All-Inorganic CsPbI2Br Perovskite Solar Cells through Energy Level Alignment. *ACS Energy Lett.* **2019**, *4* (10), 2491−2499.
(62) Qiu, F. Z.; Li, M. H.; Wang, S.; Jiang, Y.; Qi, J. J.; Hu, J. S. Strain Relaxation and Domain Enlargement via Phase Transition towards Efficient CsPbI2Br Solar Cells. *J. Mater. Chem. A Mater.* **2022**, *10* (7), 3513−3521.
(63) Xue, D. J.; Hou, Y.; Liu, S. C.; Wei, M.; Chen, B.; Huang, Z.; Li, Z.; Sun, B.; Proppe, A. H.; Dong, Y.; Saidaminov, M. I.; Kelley, S. O.; Hu, J. S.; Sargent, E. H. Regulating Strain in Perovskite Thin Films through Charge-Transport Layers. *Nat. Commun.* **2020**, *11* (1), 1514.
(64) Ma, C.; Eickemeyer, F. T.; Lee, S.-H.; Kang, D.-H.; Kwon, S. J.; Gratzel, M.; Park, N.-G. Unveiling Facet-Dependent Degradation and Facet Engineering for Stable Perovskite Solar Cells. *Science* **2023**, *379* (6628), 173−178.
(65) Zhang, X.; Ye, F.; Tu, Y. Large-Area Metal Halide Perovskite Photovoltaics Based on Solvent Bathing and Solution Bathing. *Solar RRL* **2023**, *7* (23), No. 2300618.
(66) Jang, G.; Ma, S.; Kwon, H. C.; Goh, S.; Ban, H.; Lee, J.; Uk Lee, C.; Moon, J. Binary Antisolvent Bathing Enabled Highly Efficient and Uniform Large-Area Perovskite Solar Cells. *Chemical Engineering Journal* **2021**, *423*, No. 130078.
(67) Tzoganakis, N.; Chatzimanolis, K.; Spiliarotis, E.; Veisakis, G.; Tsikritzis, D.; Kymakis, E. An Efficient Approach for Controlling the Crystallization, Strain, and Defects of the Perovskite Film in Hybrid Perovskite Solar Cells through Antisolvent Engineering. *Sustain Energy Fuels* **2023**, *7* (17), 4136−4149.
(68) Mundt, L. E.; Schelhas, L. T.; Stone, K. H. Accurately Quantifying Stress during Metal Halide Perovskite Thin Film Formation. *ACS Appl. Mater. Interfaces* **2022**, *14* (24), 27791−27798.
(69) Qian, M.; Mao, X.; Wu, M.; Cao, Z.; Liu, Q.; Sun, L.; Gao, Y.; Xuan, X.; Pan, Y.; Niu, Y.; Gong, S. POSS Polyimide Sealed Flexible Triple-Junction GaAs Thin-Film Solar Cells for Space Applications. *Adv. Mater. Technol.* **2021**, *6* (12), No. 2100603.

https://doi.org/10.1021/acsenergylett.4c01817
ACS Energy Lett. 2024, 9, 4153−4161